Toward a NASA Deep Space Optical Communications System*

Dr. Leslie J. Deutsch†, Dr. Stephen M. Lichten, Dr. Daniel J. Hoppe
Jet Propulsion Laboratory, California Institute of Technology

Anthony J. Russo, Dr. Donald M. Cornwell
National Aeronautics and Space Administration

As discussed at SpaceOps in 2016, we expect the data rates from deep space missions to increase approximately one order of magnitude per decade for the next 50 years. The first order of magnitude improvement will come from existing plans for radio frequency (RF) communications including enhancements to both spacecraft and Deep Space Network (DSN) facilities. The next two orders of magnitude are predicted to come from the introduction of deep space optical communications. Studies indicate that optical receive apertures of between 8m-12m are desired. The large cost of dedicated receive telescopes makes this method unrealistic – at least in the near-term. The cost of large optical ground terminals is driven primarily by the cost of the optics and by the cost of a stable structure for the telescope. We propose a novel hybrid design in which existing DSN 34m beam waveguide (BWG) radio antennas can be modified to include an 8m equivalent optical primary. By utilizing a low-cost segmented spherical mirror optical design, pioneered by the optical astronomical community, and by exploiting the already existing extremely stable large radio aperture structures in the DSN, we can minimize both of these cost drivers for implementing large optical communications ground terminals. Two collocated hybrid RF/optical antennas could be arrayed to synthesize the performance of an 11.3m receive aperture to support more capable or more distant space missions or used separately to communicate with two optical spacecraft simultaneously. NASA is in the midst of building six new 34m BWG antennas in the DSN. The final two are planned to be built at the DSN Goldstone, California and Canberra complexes. We are now investigating building these last two antennas as RF/optical hybrids. By delaying their operational dates by two years, we would be able to add the 8m optical receive capability for these two antennas while fitting within existing budgetary constraints. This paper describes the hybrid antenna design, the technical challenges being addressed, and plan for using this concept, together with ongoing work on optical flight terminals, to infuse operation optical communications into deep space missions.

Nomenclature

BWG	=	Beam Waveguide
CCSDS	=	Consultative Committee for Space Data System Standards
DAEP	=	DSN Aperture Enhancement Project
DSN	=	Deep Space Network
DSOC	=	Deep Space Optical Communications
DSS-13	=	Deep Space Station 13
DTN	=	Disruption Tolerant Networking
JPL	=	Jet Propulsion Laboratory
LADEE	=	Lunar Atmosphere and Dust Environment Explorer
LLCD	=	Lunar Laser Communications Demonstration
MSPA	=	Multiple Spacecraft per Antenna
OCTL	=	Optical Communications Telescope Laboratory
PST	=	Point Source Transmission
RF	=	Radio Frequency

* The research was carried out at the Jet Propulsion Laboratory, California Institute of Technology, under a contract with the National Aeronautics and Space Administration.
† Corresponding author: Phone: (818) 354-3845, Email: leslie.j.deutsch@jpl.nasa.gov

SAC = Spherical Aberration Corrector

I. Introduction

Over the next 50 years, the average downlink data rate from deep space missions will increase by an order of magnitude each decade[1]. There are many reasons for this expected increase. For one, we are ending the era of "fly-by" exploration and seeing an increase in orbiters and landers that stay for many years at their targets. There is also a trend toward higher bandwidth instruments, inheriting technology applied first in Earth observation missions. An example of this future trend is the NASA-ISRO Synthetic Aperture Radar (NISAR) instrument, which will downlink science data from Earth orbit at rates exceeding 3 Gbps, totaling more than 25 Tb/day. NASA's plans for future solar system exploration include proposed missions carrying comparable instruments to Venus, Mars and beyond to outer planets. These instruments will require very large data rates and volumes to return rich data sets from large distances. Human exploration will likely require data rates of hundreds of Mbps from Mars distance. Additionally, future missions may comprise multiple spacecraft operating as constellations to provide improved science observations.

We are currently working to improve NASA's existing radio communications infrastructure to provide the first of these additional orders of magnitude in downlink communications performance. The improvements for the first decade will come from a combination of new flight and ground systems that remove current bottlenecks[2,3], increased use of Ka-band over X-band, and newer error-correcting codes.

Optical communications will likely provide the next two orders of magnitude of performance improvement. NASA has been developing technology for deep space optical communications since the 1980s[4] when the first laboratory demonstrations of multi-bit-per-photon systems were realized. The first demonstration with a spacecraft at lunar and greater distance was accomplished with the Galileo Optical Experiment[5] (GOPEX) in 1992. GOPEX used ground-based lasers to record pulses of light on the Galileo spacecraft's camera as the spacecraft rotated during the transmission. JPL built the Optical Communications Test Laboratory (OCTL) on nearby Table Mountain in 2003[6]. OCTL has been used in many demonstrations with spacecraft in Earth orbit including the Japanese Optical Inter-orbit Communications Test Satellite and NASA's Optical Payload for Lasercomm Science[7]. More recently, OCTL was used as one of three ground terminals in the Lunar Laser Communications Demonstrator[8] (LLCD) carried to the Moon on NASA's Lunar Atmosphere Dust and Environment Explorer (LADEE) spacecraft.

LLCD, along with the future Lunar Communications Relay Demonstration[9] (LCRD) which will fly in Earth geostationary orbit, have paved the way for infusion of optical communications in Earth orbit. We expect this infusion to happen readily in the next decade because of two main things: 1) The above-mentioned demonstrations have proven the technology and retired most of the risks associated with an operational capability, and 2) the ground-based infrastructure for Earth orbiting optical communications can be accomplished with small (less than 0.5m) aperture telescopes that are both readily available and relatively inexpensive. Operational optical communications in Earth orbit is expected to achieve at least an order of magnitude improvement over existing RF systems and deliver data rates in the 10s to 100s of GB/s.

In order to infuse optical communications into the operational deep space environment, we need demonstrate the appropriate space terminal technology so as to also retire the risks associated with this class of missions. We expect this to be accomplished with the planned flight of the Deep Space Optical Communications[10] (DSOC) terminal on the Psyche[11] mission. Psyche is planned to launch in 2022 on its journey to the metallic main-belt asteroid Psyche. The DSOC demonstration will occur in the first year or two of Psyche's flight. The DSOC demonstration will use OCTL for the optical uplink and the Hale 200" (~5m) Telescope at Palomar Observatory for downlink.

Though DSOC is expected to retire the flight-side and system risks of deep space optical communications, making it ready to fly on other missions, we still need to develop an operational ground infrastructure. JPL has done analysis for NASA's ongoing next generation architecture studies that show we will need the equivalent of an 8m-12m ground telescope to support the links that are expected to be needed for human missions to Mars. The technology certainly exists to construct and operate telescopes of this size. Also, because the optical system does not require fully diffraction-limited primary mirrors, we may be able to construct these for substantially less than the cost of astronomical observatories of similar size. However, this still represents a substantial investment that would have to be accomplished before mission designers could commit to using optical communications.

An obvious alternative to building dedicated communications telescopes is to share facilities with optical astronomers. However, some requirements for the communications system – including the need to operate in both daytime and nighttime – present logistical and operational difficulties at most facilities.

Another alternative is to add optical mirrors to existing or future DSN RF antennas. This has the possibility of providing a lower cost solution, but comes with a host of interesting challenges. In fact, NASA has studied concepts for combing RF and optical systems on the same antenna structure since 2010[12]. Recent experimental work and engineering studies (described below) along with innovative funding mechanisms have resulted in such hybrid RF/optical antennas forming a major piece of NASA's current strategy for infusing operational deep space optical communications.

The following sections outline the concept in much more detail and also describe the steps necessary to advance this concept to operational reality.

II. The RF/Optical Antenna Concept

Figure 1shows the basic design of the RF/optical hybrid antenna. It is based on the design of the DSN 34m Beam Waveguide (BWG) RF antenna. BWG antennas have been operating in the DSN since 1992[13] and have proven themselves to have excellent pointing and stability.

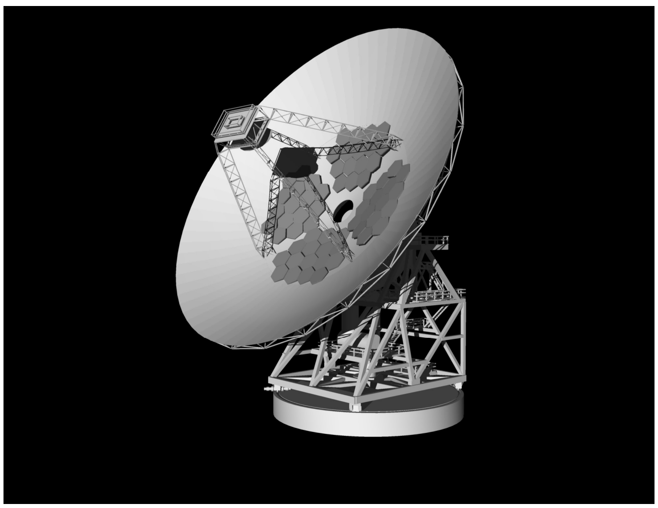

Figure 1. Concept for RF/Optical Hybrid Antennas

The basic idea of the hybrid concept is to place segmented optical mirrors on the inner area of the antenna's primary RF reflector. These would be segments of a spherical optical primary mirror. We have chosen to use a spherical primary rather than a paraboloid to reduce the cost of the system and take advantage of recent advances in spherical segmented mirrors in the optical astronomy community. These segments would be actuated on their edges to allow for figure compensation as the antenna points in elevation. Of course, this configuration necessitates a decrease in the RF performance of the antenna approximately equal to the reduced RF reflecting area.

In order to reduce stray light issues, the spherical segments would be placed to avoid reflections from the four subreflector supports. This results in the four "pod" configuration shown in Figure 1. The total area this allows is just over 50 m^2, or the equivalent of an 8m diameter monolithic mirror.

The RF subreflector mounted below the apex of the antenna would be redesigned as to illuminate only the remaining RF panels. This will leave a hole in the center of the subreflector through which the signal reflected from the optical primary can pass to a new optical processing system on the apex platform. This system would include an optical receiver along with a lens assembly for correcting the spherical aberration.

There would be no optical uplink on this hybrid antenna. Instead, a smaller (~ 1m diameter) optical station somewhere nearby would supply uplink. For the DSN Goldstone site, a 1m telescope on Table Mountain would suffice for this. In any case, the cost of these smaller stations is not a driving function in the infusion process.

The hybrid antenna would retain all of its RF capabilities, albeit at a loss of 0.6 dB resulting mainly from the loss of RF reflecting area on the primary, plus some other smaller losses that the current design minimizes. Both RF and optical signals could be received (and RF transmitted) simultaneously in operations. Hence, the one antenna could service a deep space mission with simultaneous RF and optical downlinks, further reducing the cost of operations. In principle, different spacecraft could even be serviced at optical and RF simultaneously, provided that the optical user is located within the RF field of view that includes the RF user.

When performance beyond an 8m equivalent optical aperture is required, two or more of these hybrid antennas could be arrayed. Two hybrid antennas would provide the optical performance of an 11.3m diameter telescope. We've looked at adding a larger surface area for the optical portion of the RF/Optical hybrid, but beyond 8M we would have to both increase the mass and distribute the loads outside the integral ring girder of the reflector. This would make the spherical aberration correction system more complicated and require a mechanical structure update for additional mass and moments.

III. Experiments and Studies Completed This Far

In conjunction with the design effort for the RF/Optical ground station described in the previous section, laboratory and fieldwork were undertaken in a number of key areas. In this section, we will briefly summarize this work.

In order to demonstrate the viability of using the RF antenna to track optical sources, a simple optical receiving system was installed on DSS-13, the Deep Space Network's research and developmental 34-meter beam waveguide antenna at Goldstone CA. As depicted in figure xx below, the system consists of a two-segment optical mirror assembly mounted through the RF panels to the backup structure of the antenna and a focal plane receiver mounted to the edge of the RF secondary.

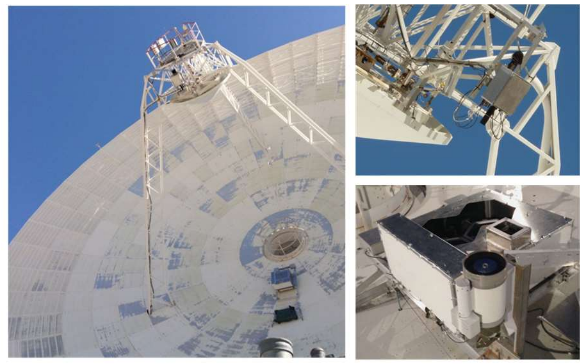

Figure 2 Optical demonstration system at DSS-13.

The mirror assembly, depicted in the right half of Figure 2, includes two hexagonal optical segments, each approximately 40 cm tip-to-tip. The radius of curvature of these spherical segments is approximately 24m, creating a focus near the edge of the RF secondary. Actuators with sub-micron resolution allow tip/tilt and piston adjustment of the mirror pair and individually tip/tilt the left mirror with respect to the right most mirror. A SiO2/TiO2 coating, suitable for the open-air environment, is applied to the segments. The assembly also includes a target camera which images the focal plane assembly and its relative motion. The focal plane assembly, depicted in the right half of Figure 3, contains a filter wheel and large primary camera (red) visible at the right most position, as well as beam splitters, a fast video camera, and a pupil camera for imaging the segments themselves. A linear stage under the assembly allows for focus adjustment.

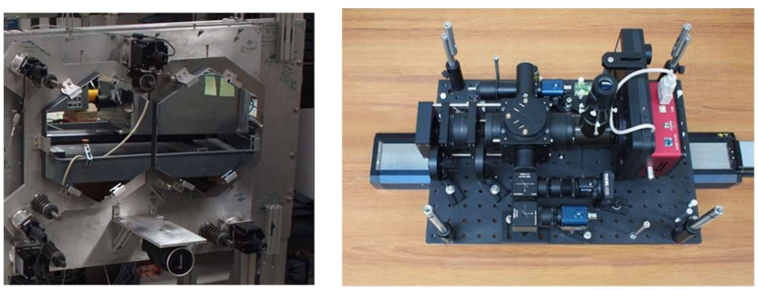

Figure 3 Mirror assembly (left) and Focal Plane Assembly (right).

The moon and combination RF/optical sources such as Saturn were used to achieve initial alignment of the optical system and co-align the RF and optical beams, as shown in Figure 4 Images taken during the initial alignment sequence. In this figure the right panel shows a dual image of Saturn is shown prior to co-alignment of the two optical segments.

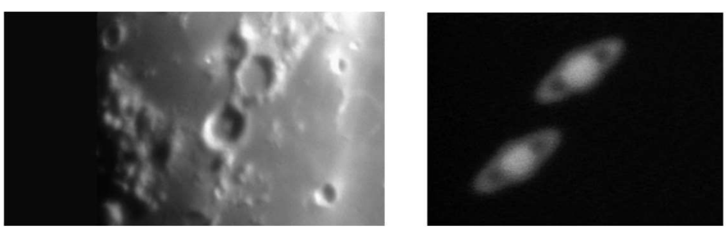

Figure 4 Images taken during the initial alignment sequence.

The DSS-13 optical system and test sequence were designed to show acquisition of the optical sources using the RF mount and pointing model, confirm the stability of the RF platform for optical tracking, and demonstrate the ability to position the mirror segments with micro-radian precision in an open-air environment.

After initial alignment, various month in a number of environmental few years. A typical sequence included RF pointing model and applying initial based on a table look-up and the source instances this simple method was both segments well into the 1 mrad Small adjustments were then made to them to the center of the field. Example Figure 5. In this image the 80% encircled energy spot size is approximately 20 micro-radians, and is determined by a combination of optical seeing and mirror segment quality. For the initial RF/Optical ground station the detector size encompasses approximately 50 micro-radians on the sky, and the goal for the experiments is to maintain the spot within this hypothetical detector throughout a typical track.

Figure 5 Images of Vega prior to co-alignment (left), and after (right).

Throughout the alignment process the ground station is of course, tracking the source using the RF pointing model. After initial alignment of the spots the co-alignment of the spots and the centroid is recorded throughout the track. Typical tracks showed a common-mode (to both segments) pointing error of several hundred micro-radians over an elevation range of tens of degrees. This is consistent with expectations based on the RF pointing model accuracy and the local tip/tilt environment of the antenna structure as a function of elevation angle [14,17]. Differential-mode pointing error (difference between segments) was typically several times smaller. This error is driven by the mechanical details such as the design of the mounts used to fasten the actuators to the segments. Figure 6 shows a typical example of differential segment pointing using the Crag Nebula as the source. In this example a differential pointing error of approximately 150 micro-radians is observed as an elevation rage of 40-60 degrees is traversed. It can be noted that the response is nearly linear, smooth, and easily corrected using the segment actuators. This result is typical of those observed throughout the test campaign.

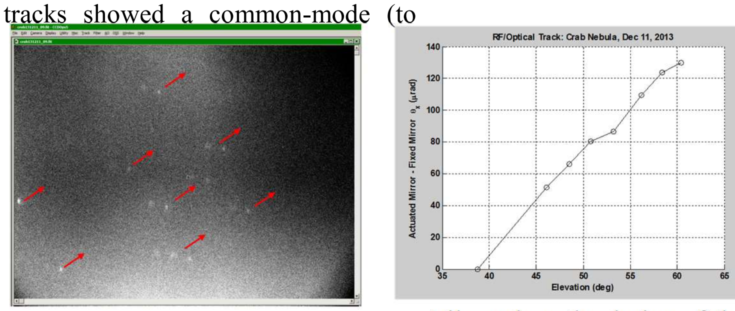

Figure 6 Differential segment pointing during a track of the Crab Nebula.

While co-alignment of the two segments in the demonstration system is a relatively simple matter, this is not necessarily the case for the full system where 64 segments are involved. Demonstration of a pupil-camera system to aid in initial segment alignment was also part of the DSS-13 experiment. The pupil-camera concept is depicted in the left-most pane of Figure 7. The pupil camera is optically focused on the segments themselves as they are illuminated by the optical source. Light from the segments passed through a variable

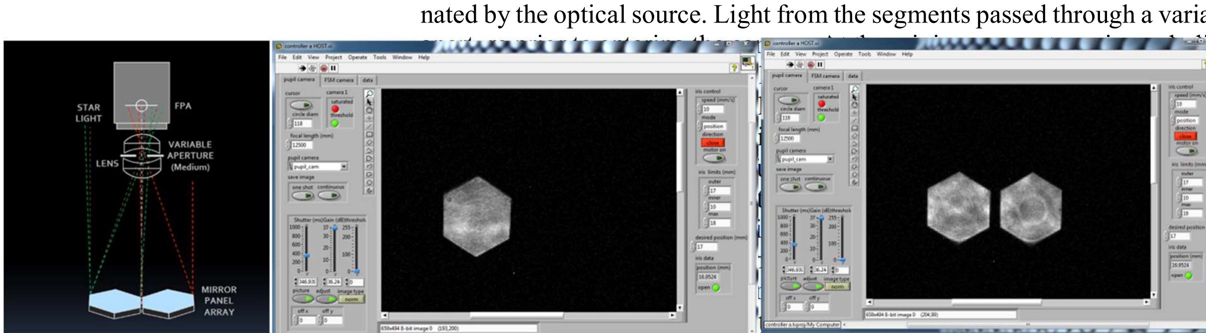

Figure 7 Pupil camera concept and sample segment images.

segment demonstration the pupil camera was used in a manual mode only. In future experiments, with more segments, we plan to fully automate the system.

Environmental conditions are a major factor in the implementation of an open-air optical communication ground station. In particular, wind can interact with the

RF primary and secondary structures and induce pointing errors. A primary area of concern is the relative position of the RF primary and secondary since each houses one of the two ends of the optical chain. Spot motion in the focal plane and direct imaging of the focal plane assembly using the target camera on the RF primary in wind can directly measure this effect. While nominal wind conditions were not significant in our ability to maintain the spot inside the 50 micro-radian detector, winds in excess of 20 Mph were significant. Figure 8 shows the first structural resonance for the antenna which is a twisting mode of the subreflector structure at approximately 2.4 Hz. The right panel of the figure plots a direct measurement of this resonance obtained by processing video images of the spot motion in the focal plane. No other significant structural resonances were observed. It should be noted that this resonance is important for our experimental system where the focal plane assembly is at the edge of the RF secondary since it causes direct lateral motion. However, for a centrally mounted optical assembly such as that in the operational design the effect of this resonance is greatly reduced.

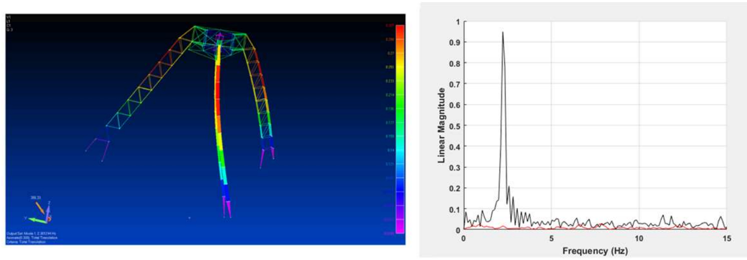

Figure 8 First structural mode of the antenna, and direct measurement of the resonance.

A fast steering mirror can easily compensate for low frequency pointing errors such as those observed in the experiments at DSS-13, and a FSM will surely be present in the aft optics of the operational system. Recently an upgraded focal plane assembly was installed at DSS-13[15]. A block diagram and photograph of the unit is shown in Figure 9. Like the first-generation assembly, the new version includes a test source, a number of beam splitters, a pupil camera, and a main camera. Additionally, the fast steering mirror is implemented requiring a collimating mirror and an additional camera to close the steering mirror loop. The system is currently on the antenna and has gone through initial alignment.

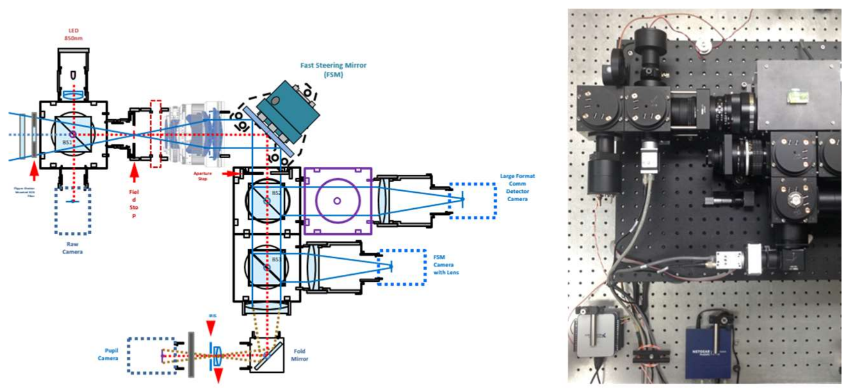

Figure 9 Second-generation focal plane assembly.

Along with the demonstration at DSS-13 there is also an on-going effort to characterize the optical channel at Goldstone[16]. The suite of instruments includes a particle profiler, night time and day time seeing monitors, a solar scintillometer, a sun photometer, a boundary layer scintillometer and a cloud camera. Many of these instruments have been in near continuous operation for several years, necessary to build up a statistical model for the channel. Early experiments were also conducted to measure the dust contamination rate on the RF primary using a group of small mirrors and a hand-held BRDF meter[14]. This information is necessary in order to determine a mirror cleaning schedule and method for the operational system.

Laboratory work in support of the RF/Optical ground station is also on-going, and includes mechanical/structural analysis, stray light analysis, optical design, and cryogenic the proposed ground station, a prime-focus optical system is ng a fully tippable 1 K cryogenic system. Photographs of an ntal sub 1 K tipping Dewar in figure xx. The system uses an K DSN Dewar with an additional 1 K absorption cooler stage. tests have validated the basic mechanical design, the cooling over the 90 degrees of elevation tipping angle, and the mechanical/optical stability of the detector mount.

Figure 10 Prototype 1 K tipping cryogenic package.

A structural/mechanical analysis of the proposed tion was performed[17]. The analysis considers the margins of the existing structure including the additional optical segments the resulting deformation of the RF surface and its impact on antenna efficiency. Figure 11 shows the Nastran model of the structure as well as computed optical segment tip/tilt and piston as a function of elevation angle. These calculations are necessary to properly size the segment actuators for the final system. Two curves are shown on each plot, one for the baseline beam waveguide (BWG) implementation and a second for an implementation on one of the DSN's high efficiency 34m antennas (HEF).

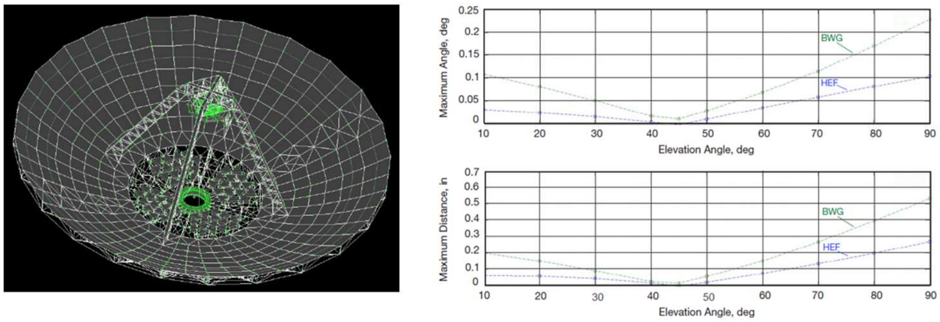

Figure 11 Structural model of the RF/Optical ground station.

As a final example of additional work on the ground station results from a recent stray light study are depicted in Figure 12. For an optical communication system, the achievable data rate is a function of the available signal power density at the ground station and the background light level seen by the detector. Stray light from the sun is one of the primary concerns when trying to track near the sun in the day. While it is not directly in the field of view of the communication detector sunlight can be scattered off of auxiliary structures into the detector. Dust contamination on the mirror segments and the raw mirror surface roughness also contribute but are mitigated by the choice of materials in our proposed design. The left panel of the figure shows the stray light model, whereas the remaining two panels show how the point source transmission (PST) for the system. The PST is the transfer function relating the detector power density to plane wave source density incident from a given direction. In the center panel for source angles near the main optical direction (< 1 degrees) the PST is a monotonically rising function, dominated by stray light from the segment contamination and roughness. For larger angles the PST is nearly constant and dominated by light hitting the RF primary near the optical segments and leaking into the detector. This path from the RF primary can be eliminated by an appropriate stop in the optical train. This is depicted in the

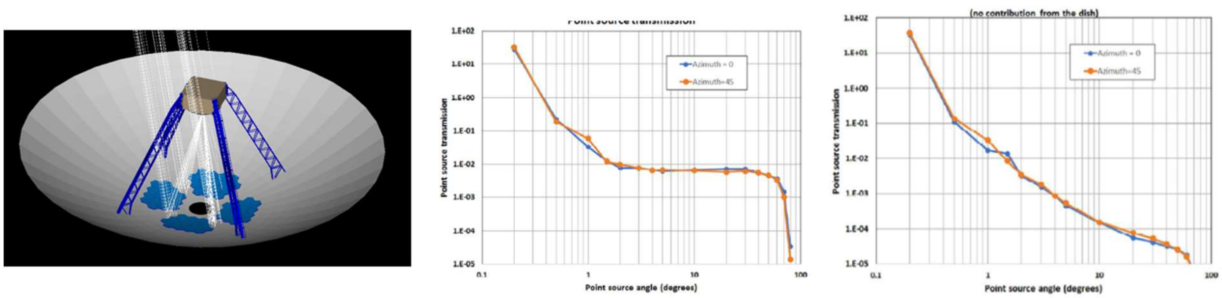

Figure 12 Stray light analysis of the RF/Optical ground station.

results on the rightmost panel of the figure.

IV. Plan to get to the First Operational Unit

There are four key steps for prototyping, field testing, and implementing the first hybrid RF-Optical aperture in the DSN:

- A a seven-element small mirror prototype in DSS-13;
- B a 16-element pod in DSS-13 with full size mirrors and receiver/demodulator;
- C a complete 4-pod, 64-element optical ground terminal in DSS-13; and
- D transfer of complete 64-element system into an operational 34m DSN antenna at the Goldstone tracking complex.

For each of these four steps, a complete battery of field tests is planned in a relevant environment, including daytime and nighttime operation, over extended periods so that a full range of weather and seasonal conditions are experienced.

A. 7-Element Prototype Demonstration in DSS-13

While the initial demonstrations at DSS-13 with the pair of 0.4m mirrors were sufficient to show the compatibility of the RF mount with requirements for an optical communication ground station, additional field tests are required to demonstrate key needed capabilities. For example, we need to demonstrate the ability to keep a large number of optical segments aligned with their parent sphere without optical feedback. Bright sources in the vicinity of a spacecraft may be initially used to align the segments, but once the antenna is slewed to the spacecraft there will not be sufficient signal photons to maintain segment alignment. Thus, an autonomous closed-loop segment alignment system consisting of edge sensors, actuators, control loop, and associated computer system will be engaged once initial alignment is complete. A second-generation prototype demonstration system to be installed at DSS-13 is currently under development. The system is depicted in Figure 13.

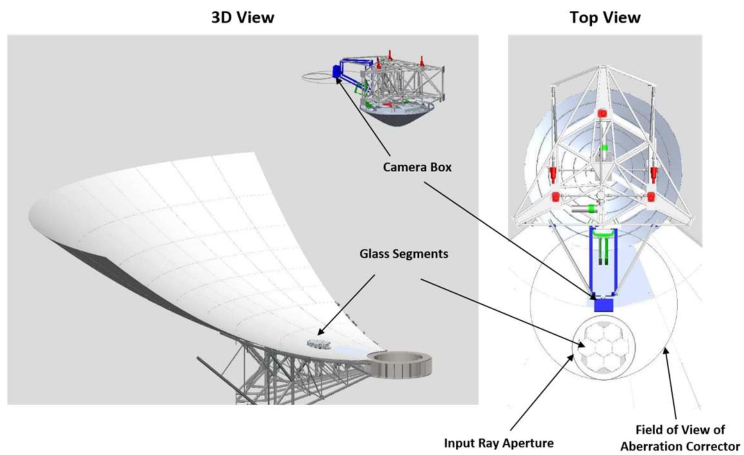

Figure 13 Second-generation DSS-13 optical demonstration with seven-segment prototype.

As can be seen in the figure, the second-generation prototype system includes seven segments on the RF primary inside DSS-13, and a focal plane assembly mounted off the RF secondary as before. The seven segments are each 0.5 m tip-to-tip, slightly larger than the 2-element demo segments, and are also segments of a parent sphere with a radius of 24 m. The larger spherical collecting area would produce a spot well in excess of the desired 20 micro-radian spot size due to spherical aberration. Thus, for this demonstration, a custom spherical aberration corrector (SAC) will be added to the front of the second-generation focal plane assembly shown in Figure 14. As shown in the Figure the optical arrangement is such that the incoming rays are unblocked by the focal plane assembly, and the mirror segments fall within the correctable range of the SAC. The seven mirror segments will be fully actuated and outfitted with edge sensors. Autonomous alignment control of the segments after initial alignment on a suitable source will be demonstrated in an open-air environment in a DSN 34m aperture, retiring key remaining risks for the RF/optical ground station concept. The corrector is a custom design, employing three large 120 mm lenses and a small field-flattener. Preliminary testing of the SAC is complete and indicates nominal performance. Additional testing is planned. The SAC is able to correct for the spherical aberration over approximately a 3 m diameter circle. As configured, the seven segments are inside of, but not centered on this circle when viewed from the focal plane. This is necessary to avoid blockage, but a large amount of correctable, but unused area remains available for the future.

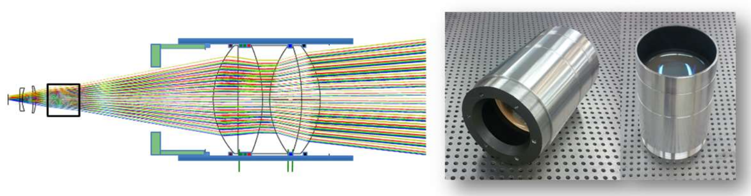

Figure 14 Spherical aberration corrector.

Finally, Figure 15 shows seven 0.5m hexagonal segments configured on an optical bench. Eight segments have been procured and received, allowing for one spare. The coating on these segments is the same durable coating currently in use at DSS-13. The segments include the necessary features on the rear surface to mount the edge sensors, two per edge. In-house testing of the segments to verify vendor measurements of focal length and image quality is currently in the planning stage.

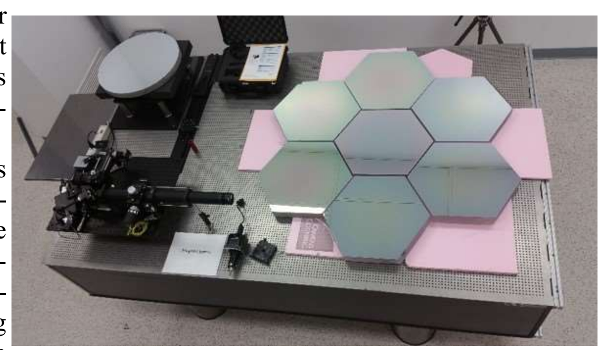

Figure 15 Second-generation 0.5 meter mirror segments.

Completion of the seven-element prototype and field tests covering a full cycle of seasons in the relevant outside environment in a DSN 34m BWG antenna could be accomplished within about two years.

B. 16-element Single Pod Implementation and Field Test in DSS-13 with Full-Size 1.1m Mirrors

Following the successful seven-element small-mirror prototype demonstration in DSS-13, the next step toward an operational DSN hybrid RF-Optical ground terminal is the implementation and field test of a "pod" in DSS-13, consisting of 16 full-size 1.1m mirror segments. The 16 mirrors will provide an equivalent optical aperture of 4.1m, and this field test will completely test one of what would eventually be four pods (64 mirror segments) for the complete operational aperture. In contrast to the seven-element field test, the 16-element pod comprises the first quarter of what would eventually become an operational 8m equivalent optical aperture. Figure 16 depicts the four pods installed within a DSN 34m BWG antenna. The 16-element field test would be conducted with the first, single pod installed in DSS-13 at the NASA Goldstone tracking complex.

The 16-element field test will include an optical communications receiver for demodulation of optical communications data sent from a spacecraft still to be determined. One implementation option, funding permitting, would have the 16-element pod ready for use in DSS-13 by mid-FY23, about two years after completion of the seven-element prototype task. This would be in time to receive optical communications from DSOC on the Psyche mission.

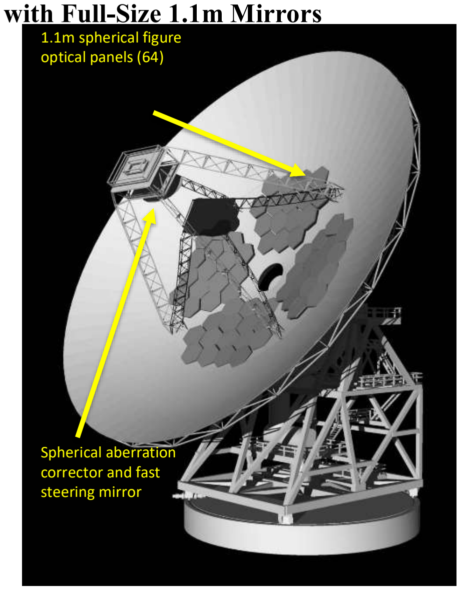

Figure 16 Depiction of complete 64-element, 4-pod operational hybrid RF-Optical aperture with 8m of optical collecting area inside a DSN 34m RF antenna

C. 64-element 4-Pod Implementation and Field Test in DSS-13 with Full-Size 1.1m Mirrors

Following successful completion of the single pod 16-element field testing in DSS-13, the next phase of the hybrid aperture implementation will include procurement and installation of the remaining 48 mirrors to complete the 64-element hybrid RF-Optical aperture. Testing of the complete system will then proceed, preferably with signals from an active spacecraft. This phase may take up to two years, including extended field tests in an operational relevant environment.

DSS-13 serves as a good "proxy" for an operational DSN 34m BWG antenna, with one difference. The subreflector on DSS-13 is supported by a tripod structure, versus a quadrapod structure on the operational 34m BWG antennas. The final 64-element 4-pod system fits naturally under the quadrapod (Figure 13) with minimal shadowing or reflections from the four subreflector support legs. For an operational implementation we will use 4 pods snuggled between each of the legs. Since DSS-13 has only three support legs for the subreflector, while we will likely still use 4 pods at DSS-13, we will likely not populate those sections of the pods that fall under the legs of the tripod with mirrors. Instead a non-reflective material will be used for those sections so as not to see scattered light, but the system will still carry the edge sensor system throughout the entire set of four pods. The result is that there will be a somewhat reduced optical area for the DSS-13 64-mirror system, but it will be enough to do the necessary prototyping and field demonstrations. When we transfer the full optical system from DSS-13 to the operational 34m BWG antenna, we will populate all the mirror locations.

D. Transfer of 64-element 4-Pod System from DSS-13 to An Operational DSN 34m Antenna

The final phase of the implementation for the first hybrid RF-Optical aperture in the DSN will be the transfer of the complete 64-element system of full-size 1.1m mirrors from the research and development DSS-13 aperture into an operational DSN 34m aperture. Nominally, this could be accomplished within 6 months, moving the first such optical system into what will then be a new DSN Goldstone 34m antenna, DSS-23. Subsequent 8m optical apertures could be developed in about 20 months and installed into either new or existing DSN 34m apertures at any of the three DSN complexes.

V. Funding Mechanisms

While the use of the hybrid RF/optical antennas will certainly reduce the cost of emplacing an operational capability for deep space optical communications in the DSN, it still does not come for free. In fact, even the current project to construct new 34m BWG antennas is being accomplished without additional NASA funds. This is possible because of recent advances in automation that have resulted in significant operations efficiencies in the DSN.

Two major operational efficiencies have already been completed. The first of these is known as "Two Links per Operator[18]." As the name implies, DSN operators now typically operate two links at a time. These links and be one or two-way, so they include both uplink and downlink. This has been enabled through the gradual upgrading of DSN systems to support the required level of autonomy. Additionally, we have improved the console user interfaces to provide operators with more timely and relevant information on the links and their associated subsystems.

The second major efficiency improvement is known as "Follow the Sun[16]" or FoTS. This has been operational since November 2017. Under FoTS, each of the three DSN sites is staffed with operators for 10 hours – coinciding with daytime at the corresponding longitude. During these 10 hours, the operators at the "daylight" site control the antennas for the entire DSN. This was enabled by a combination of improved automation, advances in remote operations, and cooperative agreements among the three countries involved.

One more major efficiency is planned and will be accomplished over the next few years. This is an extension of "two links per operator" to "three links per operator." This is work in progress.

These efficiencies have provided a funding wedge in the DSN budget that has enabled the ongoing DSN Aperture Enhancement Project[19], or DAEP. Under DAEP, we are constructing six new 34m BWG antennas. So far, two new antennas have been completed at the Australia site and two have begun construction in Madrid. When completed, the six new antennas will provide

- additional aperture in the Southern hemisphere to help balance sky coverage
- additional Ka-band (both 26 GHz and 32 GHz) capability to help enable increased performance and
- the ability to provide an operational backup for the 70m antennas at each site.

The current concept is to convert the final two DAEP antennas into hybrid RF/optical systems. We estimate that, by delaying the schedule for these two antennas by approximately two years, we can use the budget wedge created by the above efficiencies to fund the additional cost of the hybrid system. The deferred costs of the final two DAEP antennas will be addressed in future budget cycles and NASA has sufficient Deep Space capacity to meet user needs until they come online. In this way, we hope to create the first two hybrid 34m RF/optical antennas without a significant impact on the DSN budget.

This would not be possible if we were to build monolithic 8m class telescopes. We looked at historical examples such as the Large Binocular Telescope (two 8.4m standalone optical apertures), the Gran Telescopio Canarias (10.4m standalone optical aperture), and the Keck 10m telescopes, as well as a recent JPL study of what it would take to build a new standalone optical aperture today. In all cases, the cost of the hybrid was less than half of what we would expect to pay for monolithic system with the savings achieved by leveraging the existing and planned Deep Space infrastructure. It also allows us to retain significant RF capability which will still be required even as we transition some services to optical.

In addition, we considered attempting to meet NASA's evolving Deep Space mission needs through expansion of the existing RF infrastructure but concluded we would need an additional four to six 34m antennas per site. The current mission models indicate both an increase in the number of missions and the data rate requirements of those missions as we approach the Mars human exploration era. Meeting these evolving needs with a traditional RF approach would require an additional investment of more than billion dollars above the current baseline of the Deep Space Network. The hybrid concept allows us an earlier capability, performance advantages and a significantly reduced overall cost.

VI. Link Calculations for the Mars Example

In this section, we examine the feasibility of enabling anticipated NASA human missions at Mars using a combination of the 34m hybrid RF/optical antenna and a second-generation deep space optical flight terminal.

When Mars in in the portion of its orbit when it is close to the Earth (and in the night sky), the optical system can support a very hefty data rate. Hence, we concentrate on the worst case to get a lower bound on the downlink data rate for these missions. The worst case occurs when Mars in near conjunction and sits close to the Sun in the sky as seen from the Earth.

We expect the DSOC terminal downlink to the 200" (~5m) Palomar Observatory to achieve ~1.2 Mbps at 2.62 AU[20], equivalent to the farthest distance between Earth and Mars for such missions. Of course, we cannot actually use this link within ~3° (the exact angular distance is still to be determined) of a Mars conjunction, but excluding these periods, 1.2 Mbps is a good estimate.

A second-generation deep space optical communications terminal would have something like a 50 cm aperture as opposed to the 22 cm used on DSOC. Additionally, we can expect higher powered lasers on human-rated mission. We will assume 50W, as opposed to the 4W on DSOC. This could be a single laser at 1550 nm or we could use a multiplexed system with several lasers on separate wavelengths if necessary. The performance would be equivalent in either case. Together, this would provide an increase in performance of about 64.6 over DSOC, for a downlink data rate of ~77.5 Mbps into a Palomar-equivalent receive aperture.

The 34m hybrid RF/optical antenna would provide an 8m equivalent aperture, or an increase in receive performance of ~2.6 over the Palomar telescope. This additional performance gain would result in an overall downlink data rate of ~198 Mbps from Mars farthest distance.

Recent studies of what downlink data rates may be required for human Mars missions have indicated ~250 Mbps. This would be accomplished by downlinks from two relay (or one relay and one crewed) spacecraft from Mars vicinity, each with a downlink of 125 Mbps. A single 34m hybrid antenna could support 125 Mbps with 2 dB of margin. A pair of these antennas, either arrayed with a single Mars transmitter or tracking a pair of spacecraft that in turn provide relays to the human missions, can provide the total 250 Mbps with the same 2 dB of margin. Alternatively, a single hybrid antenna can support the entire 250 Mbps if it is equipped with two optical detectors, with slightly different wavelengths using multiple spacecraft per antenna (MSPA) tracking.

VII. Conclusion

The use of 34m hybrid RF/optical antennas can provide a cost-effective mechanism for the infusion of operations optical communications in deep space missions. Preliminary demonstrations using the DSN's DSS-13 antenna have shown the technical feasibility of the concept from a stability and performance viewpoint. Engineering studies thus far have further indicated that the 34m BWG antennas will have the required structural integrity to support the additional mass of the optical systems and that the stray light properties will suffice.

We have presented a plan for using DSS-13 for additional demonstrations leading directly to a first operation system that can be transferred to a new BWG antenna. These demonstrations, together with additional studies will reduce remaining risks to an acceptable level.

Finally, we have developed a plan to modify the construction schedule for the DAEP build of additional 34m BWG antennas in such a way as to offset most of the costs of the first operational hybrid system.

All of this, together with the development of the space segment of the link through DSOC on the Psyche mission, indicates a sound infusion path for optical communications in deep space in time for enabling human missions to Mars by the mid 2030s.

References

[1] Deutsch, L., Townes, S., Liebrecht, P., Vrotsos, P., and Cornwell, D., "Deep Space Network: The Next 50 Years," SpaceOps 2016.

[2] Pugh, M., Kuperman, I., et al, "The Universal Space Transponder: A Next Generation Software Defined Radio," Transactions of the IEEE Aerospace Conference, 2017.

[3] Davarian, F., "The Deep Space Network in the Common Platform Era: A prototype Implementation at DSS-13," TTC-2013, Darmstadt, Germany, September 2013.

[4] Katz, J. "2.5 Bit/Detected Photon Demonstration Program: Phase II and III Experimental Results," TDA Progress Report 42-70, Jet Propulsion Laboratory, May and June 1982.

[5] Wilson, K., and Lesh, J., "An Overview of the Galileo Optical Experiment (GOPEX)," TDA Progress Report 42-114, August 15, 1993.

[6] Wilson, K., Page, N., Wu, J., and Srinivasan, M., "The JPL Optical Communications Telescope Laboratory (OCTL) Test Bed for the Future Optical Deep Space Network, AAS 00-000, 2003?

[7] Morris, M., Kovalik, J., Andrews, K., Abrahamson, M., and Biswas, A., "Adaptive optics correction into single mode fiber for a low Earth orbiting space to ground optical communication link using the OPALS downlink," Optics Express, 2015

[8] Boroson, D., Robinson, B., Murphy, D., Burianek, D., Khatri, F., Kovalik, J., Sodnoik, Z. and Cornwell, D., "Overview and Results of the Luna Laser Communication Demonstrator," Proceedings of SPIE 8971, Free-Space Laser Communication and Atmospheric Propagation XXVI, 2014.

[9] Israel, D., Edwards, B., and Staren, J., "Laser Communications Relay Demonstration (LCRD) Update and the Path Towards Opitcal Relay Operations," Transactions of the IEEE Aerospace Conference, 2017.

[10] Biswas, A., Kovalik, J., Srinivasan, M., Shaw, M., Piazzolla, S., Wrigh,t M., Farr, W., "Deep Space Optical Communications," Proceedings SPIE, Volume, 9739, 2016.

[11] Polanskey, C., "Psyche Mission: Scientific Models and Instrument Selection," Transactions of the AGU, 2017.

[12] Vilnrotter, V., "Hybrid RF/Optical Communications via 34-meter DSN Antennas," IPN PR 42-180, pp. 1-28, February 15, 2010

[13] Bathker, D., Veruttipong, W., and Otoshi, T., "Beam-waveguide Antenna Performance Predictions with Comparisons to Experimental Results," IEEE Transactions on Microwave Theory and Techniques, Vol. 40, Issue 6, June 1992.

[14] Hoppe, D., Charles, J., Piazzola, S., Amoozegar, F., Britcliffe, M., and Hemmati, H., "Integrated RF/Opitcal Ground Stations Technology Challenges," IPN Progress Report 42-181, May 15, 2015.

[15] Hoppe, D., Chung, D., Kovalik, J., Gama, E., and Fernandez, M., "RF/Optical Demonstration: Focal Plane Assembly," IPN Progress Report 42-207, November 15, 2016.

[16] Piazolla, S., Wu, J., Franco, M., and Hoppe, D., "Preliminary Assessment of the Atmospheric Optical Channel at Goldstone (CA)," 2011 International Conference on Space Optical Systems and Applications (ICSOS,) 2001.

[17] Torrez, T., "RF/Optical Hybrid Antenna," IPN Progress Report 42-201, May 15, 2015.

[18] Statman, J. and Berner, J., "Deep Space Network – Paradigm Changes for Cost-Efficiency," Transactions of SpaceOps 2016.

[19] LaBelle, R. and Buu, C., "Uplink and Downlink Electronics Upgrades for the NASA Deep Space Network Aperture Enhancement (DAE) Project," Transactions of SpaceOps, 2014.

[20] Biswas, A., Kovalik, J., Srinivasan, M., Shaw, M., Piazzolla, S., et al., "Deep Space Laser Communications," Proceedings of SPIE, 2016.